

Damage evaluations of oven-dried mortar subjected to one-directional fire

Onnicha Rongviriyapanich*, Yasuhiko Sato and Withit Pansuk

(Received: January 27, 2016; Accepted: May 9, 2016; Published online: July 05, 2016)

Abstract: Concrete structures can be damaged by various factors in extreme service conditions. Analytical methods that can predict the strength of structural concrete after exposure to fire are needed to facilitate decisions regarding whether to repair, strengthen, or demolish fire-damaged buildings. However, appropriate and widely applicable material models have not yet been proposed. This paper presents an experimental study in which we assess damage, including changes in flexural strength, porosity and residual cement hydrates, to oven-dried mortar that has been fired and immediately cooled in the air. Mortars were made from calcareous and siliceous aggregates, and one face of each specimen (100×100×400 mm) was exposed to fire curves of ISO 834 and ASTM E119. Specimens for quantitative assessment were hewed to ten layers from the original specimens. Experimental results indicate that the in-depth flexural strength of a thin specimen is substantially diminished by fire exposure, especially for specimens with existing fire cracks. In addition to the loss in strength, changes in porosity and chemical properties occur. Based on the experimental evidence obtained from this study, the relationships between each property are discussed.

Keywords: mortar, fire exposure, fire damage assessments, meso-scale material properties.

1. Introduction

Cementitious materials, such as cement paste, mortar or concrete, are among the most popular construction materials because they have a high benefit/cost ratio, can be cast in various shapes and sizes and are non-combustible [1]. The performance of such materials varies with mix proportion, such as the cement content, aggregate type, additives and water consistency, and with the service conditions. During its service life, structural concrete deteriorates owing to various factors and structures that are exposed to severe conditions such as fires are especially vulnerable to such deterioration [2-5]. Fire is one of the most extreme conditions to which structural concrete can be exposed, and can induce severe and devastating deterioration [6,7]. Because cementitious material has low thermal conductivity and is non-combustible, it is considered to protect steel reinforcements against fire. When a structure is exposed to fire, concrete properties, including chemical structure, physical appearance and

mechanical strength, deteriorate, because concrete is designed and built without fireproofing systems [8-15]. As a result, the overall performance of a fire-damaged concrete structure is thought to be diminished. To ascertain whether a fire-damaged concrete structure should be repaired, strengthened or demolished, its residual integrity must be well examined.

Although it is widely known that cementitious material is substantially damaged by fire exposure, few studies have investigated techniques used to predict structural performance. Such techniques are powerful and have a wide range of applications. To develop such models, knowledge of the relationships between the mechanical strength and basic properties of cementitious materials is needed. Heating above 300 °C causes micro cracking to occur and propagate continuously; cracking becomes visible at approximately 400 °C, and then spalling occurs when the temperature is greater than 1,200 °C [14,16]. When the temperature is sufficiently high, the physical damage coincides with the decomposition of cement hydration products, leading to a decrease in material strength [9-11,17]. Consequently, the classical method of strength evaluation may not be able to measure the actual damage to a cementitious material after a fire, especially for one-directional fire exposure, where the degree of deterioration depends on the distance

Corresponding author O. Rongviriyapanich is a Ph.D. candidate, Graduate School of Engineering, Hokkaido University, Hokkaido, Japan.

Y. Sato is an Associate Professor, Hokkaido University, Hokkaido, Japan.

W. Pansuk is an Associate Professor, Chulalongkorn University, Bangkok, Thailand.

from the fire origin. In principle, the damage characteristics vary with several factors, including thermal loading and the mineral structure of raw materials. Carbonate and siliceous concrete show different degrees of deterioration in response to fire [18-21], but very few data are available regarding the importance of mineral structure. Fire causes damage through three main mechanisms: differences in thermal characteristics between mortar and coarse aggregate, the effects of pore pressure, and chemical compound decomposition [22]. Therefore, oven-dried mortar specimens were used in this study to prevent additional cracks introduced by a thermal mismatch between the mortar phase and the coarse aggregate or by developing pore pressure during the fire tests.

The aim of the present paper is to understand how damage to mortar progresses after one-directional exposure to fire. Generally, the performance of structural concrete is evaluated by the average response. However, uni-directional firing could introduce a non-uniform damage distribution along a specimen's depth. Therefore, the response of a meso-scale specimen could show the degree of deterioration more precisely. Although concrete is more widely used as a typical construction material, it could be difficult to clarify the fire damage mechanisms. Moreover, mortar is also used as a finishing material, and would therefore be the first material to be exposed to fire. In this study, the damage characteristics of oven-dried meso-scale mortar specimens after fire exposure are therefore investigated. Fire-damaged mortar prisms, with dimensions 400 mm in length and 100 mm in width and thickness, are used to assess cracking, residual chemical composition, porosity, and flexural strength. At the end of this paper, the fire damage characteristics and their relationships will be discussed based on the current experimental study.

2. Experimental procedures

2.1 Materials and mix proportions

The raw materials used in this study are locally available in Japan and Thailand. The ordinary Portland cement (OPC) conforms to ASTM C150 and the Thailand Industrial Standard (TIS). The fine aggregates, i.e., crushed limestone and natural river sand, are locally and widely used in Japan and Thailand, respectively. The aggregate is fine, uniformly graded sand that has passed through a 1.70-mm mesh sieve.

In this study, we used non-air-entraining mortars based on the absolute volume of the material constituents in a saturated surface dry condition that has a water-to-cement ratio of 0.55 and a cement-

to-sand ratio of 0.50. The designated mix proportions in this study, as shown in Table 1, are exactly the same for all mortar series made from raw materials locally available in both Japan and Thailand.

Table 1 – Mix proportions per cubic meter

Ingredient	Specific gravity	Amount (kg)
Cement	3.16	624
Fine aggregate	2.71	1248
Water	1.00	343

2.2 Specimen fabrication and curing regime

The 100×100×400 mm prismatic specimens were cast for the one-directional fire test. First, cement and fine aggregate were dry mixed to ensure a uniform distribution before being hydrated by water in the mix proportion. After being mixed well, the fresh mortar was poured and compacted in a 100×100×400 mm prismatic mold. It was then kept in the mold for 24 hours. As shown in Fig. 1, thermocouples were embedded during casting at various depths, e.g., 25 mm, 50 mm and 75 mm from the bottom surface. Two types of surfaces for the specimen, called the heated face and the side face, are considered. The heated face is the bottom face of the specimen, where the fire is loaded, while the side face is perpendicular to the heated face.

After demolding at 24 hours, the specimens were cured in lime-saturated water for 27 days. Next, they were oven dried at 105 °C for 24 hours to release all residual free water in the capillary pores, which causes pore pressure buildup during the fire test [23], and to keep the moisture content constant until the fire test date. These regimes provided well-cured specimens and minimized any effects of accelerated hydration and unexpected damage characteristics when heated. By using the embedded thermocouples and two thermocouples attached to the heated and unheated surfaces, thermal gradients during the entire period of burning could be measured.

2.3 Heating and cooling regimes

The specimens were one-directionally heated using a furnace programmed with the standard fire curves of ISO 834 and ASTM E119, as shown in Eqs. (1) and (2), respectively, and then cooled to ambient temperature. Fire tests were simulated for three durations (30, 60 and 90 minutes). When the targeted duration was reached, the furnace was automatically switched off, the doors opened immediately, and the specimens were left to cool in the air over many hours to room temperature, as shown in Fig. 2.

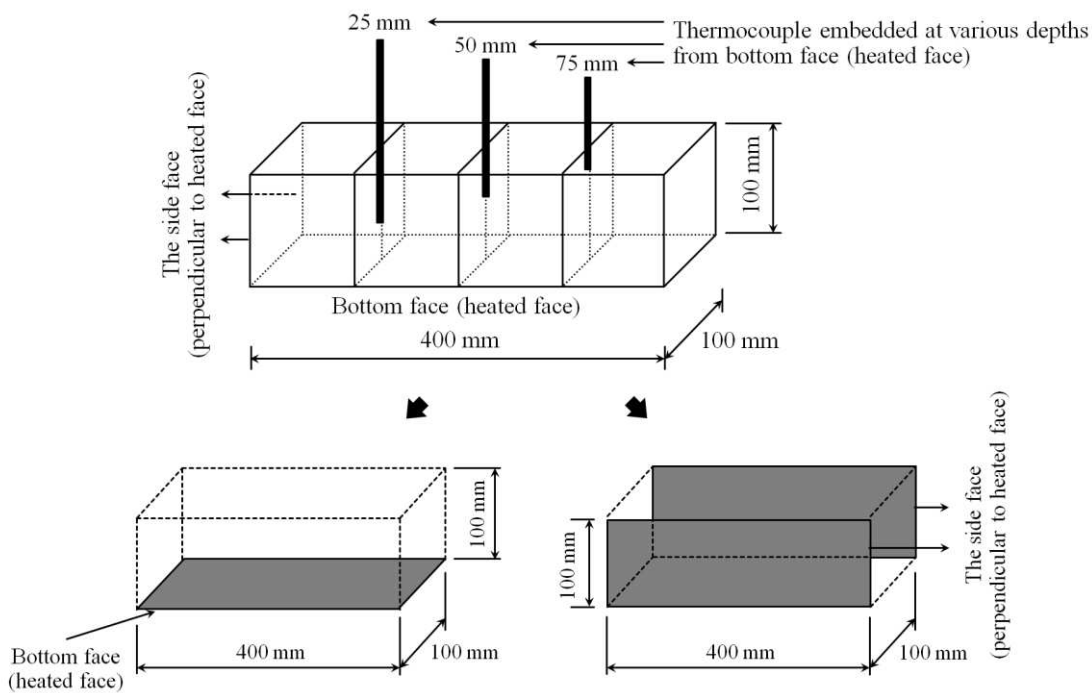


Fig. 1 – Details of specimens and surface types

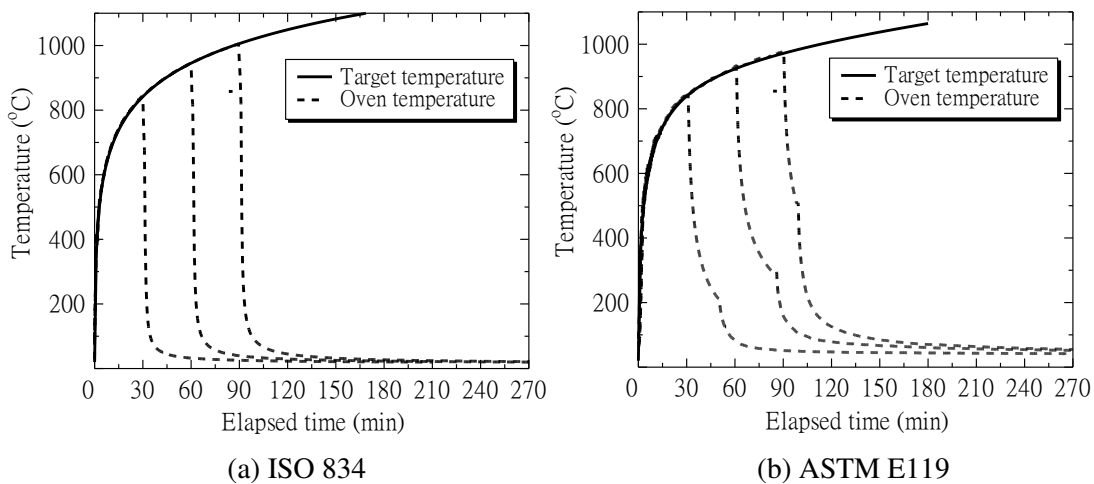


Fig. 2 – Target and oven temperature



(a) ISO 834



(b) ASTM E119

Fig. 3 – Experimental conditions of fire test

Table 2 – Specimen details

Series name	Cement	Fine aggregate	Firing	Experimental condition
JP ISO	C1	Calcareous base	ISO 834	1D without fireproof
JP ASTM	C1	Calcareous base	ASTM E119	1D with fireproof
TH ASTM	C2	Siliceous base	ASTM E119	1D with fireproof

Note: 1. C1 and C2 are cements that are locally available in Japan and Thailand, respectively; 2. All series were subjected to fire for 30, 60 and 90 minutes; 3. The quantitative damage assessments were conducted with only the series of JP ISO.

Table 3 – Unit weight of specimens

Series name	Unit weight (kg/m ³)		Loss of free water (kg)
	Saturated surface dry	Oven dry	
JP ISO	2290	2092	198
JP ASTM	2255	2136	119
TH ASTM	2154	1968	186

However, the experimental conditions of fire tests under ISO 834 and ASTM E119 were slightly different owing to the configurations of the furnace. Fireproof material was used to protect all faces of the specimens except the heated face before being left inside the furnace programmed with ASTM E119. On the other hand, the fireproof material was not necessary for specimen which was burnt with fire curve of ISO 834 because they were placed at the lid of the furnace. The details of raw materials made of mortar, as well as the standard fire curves and experimental conditions, are summarized in Fig. 3 and Table 2.

$$T = 345 \log(8t + 1) + T_0 \quad (1)$$

$$T = 750 \left[1 - e^{-3.79553\sqrt{t}} \right] + 170.41\sqrt{t} + T_0 \quad (2)$$

where T and t represent temperature (°C) and elapsed time (minutes for ISO and hours for ASTM curves), respectively. The ambient temperature is indicated by T_0 .

Because all of the mortar specimens were oven-dried to prevent the buildup of pore pressure, the unit weights of the saturated surface dry and oven-dried specimens are different as shown in Table 3.

2.4 Equipment and procedure for flexural test

The first tests of the fire-damaged 100×100×400 mm specimen involved visual inspection of physical appearance, such as surface

crack mapping. These preliminary observations allowed us to understand the damage to the materials after exposure to fire, and they were also useful for further experimental work, such as eliminating a major crack in the specimen for a meso-scale 3-point flexural test. Then, the original specimens were cut into four 100×100×100 mm cubes, and the internal cubes were sliced into thin specimens (approximately 10 mm thick) following the geometry recommendations of the Japan Concrete Institute Standard: Method of test for fracture energy of concrete by use of notched beam, JCI-S-001-2003. In total, 10 layers, from heated to unheated faces, were created to understand the non-uniform degree of deterioration along the beam depth induced by one-directional fire. Additionally, the visible damage on the top and bottom of the thin specimens was also observed.

As mentioned before, quantitative damage assessment of flexural strength, porosity, and residual chemical compounds has previously been conducted using only the JP ISO series. Figure 4 shows the use of a specimen hewed from the original prism for quantitative damage assessment. The thin specimen was first used for the bending test. Approximately 10×10×10 mm cubes were extracted from both sides of the bending failure location for the porosity test, while the remaining part was ground into a powder with a diameter of approximately 150 μm for chemical testing. In the 3-point bending test, a single point load, with a constant displacement rate of 1 μm/s, was applied to the top fiber at mid-span, and three LVDTs were installed at the middle and both ends during the entire period. A schematic bending process is shown in Fig. 5.

rosity, cement hydrates, and thermal exposure, are discussed. This technique uses new knowledge about the relationships between mechanical and physico-chemical characteristics, which have already been proposed [24]. In reference 24, it was shown that the mechanical characteristics of mortar were diminished by calcium leaching and strongly related to the amount of cement hydrates and porosity changes.

3.1 External thermal loadings and developed temperature histories

During the fire tests, temperatures were measured at several different locations in real time, such as the temperature of the oven and the surface and the developed internal temperature at the embedded thermocouples. Although one of the surfaces was directly exposed to fire, the temperature that was measured at the heated face of the specimen might not have been equal to the internal temperature of the oven for several reasons, such as thermal conductivity, the heat absorption of cementitious material, and the stability of the fire and furnace. Therefore, the temperature of the heated surface is a more appropriate value for describing the developed thermal gradients along a cross section rather than the oven's temperature.

When mortars were subjected to one-directional fire exposure, the internal temperature gradients started to gradually increase with elapsed exposure time. At a given distance from the heated face, the temperature tends to be higher when subjected to a longer duration. Along the cross section, the developed temperature gradually decreases at a greater distance from the heated face. Figure 6 shows the maximum internal temperature measured at each depth for all series. In the case of calcareous mortars, the developed temperature gradients were approximately similar despite being exposed to different temperature histories. For 30 and 60 minutes under firing, the developed temperatures had approximately the same tendencies in all mortar series. However, there were prominent differences between series when the exposure time was 90 minutes.

As seen from the developed temperature gradients, the types of raw material used in mix proportions, rather than the external thermal loading, might play a dominant role in the development of internal temperature, especially for long-term exposure. For cementitious materials exposed to fire, the initiation and propagation of a crack and its intensity probably cause a non-uniform temperature gradient along the cross section [14,25]. Therefore, the significant difference in temperatures between calcareous and siliceous mortar under the same fire

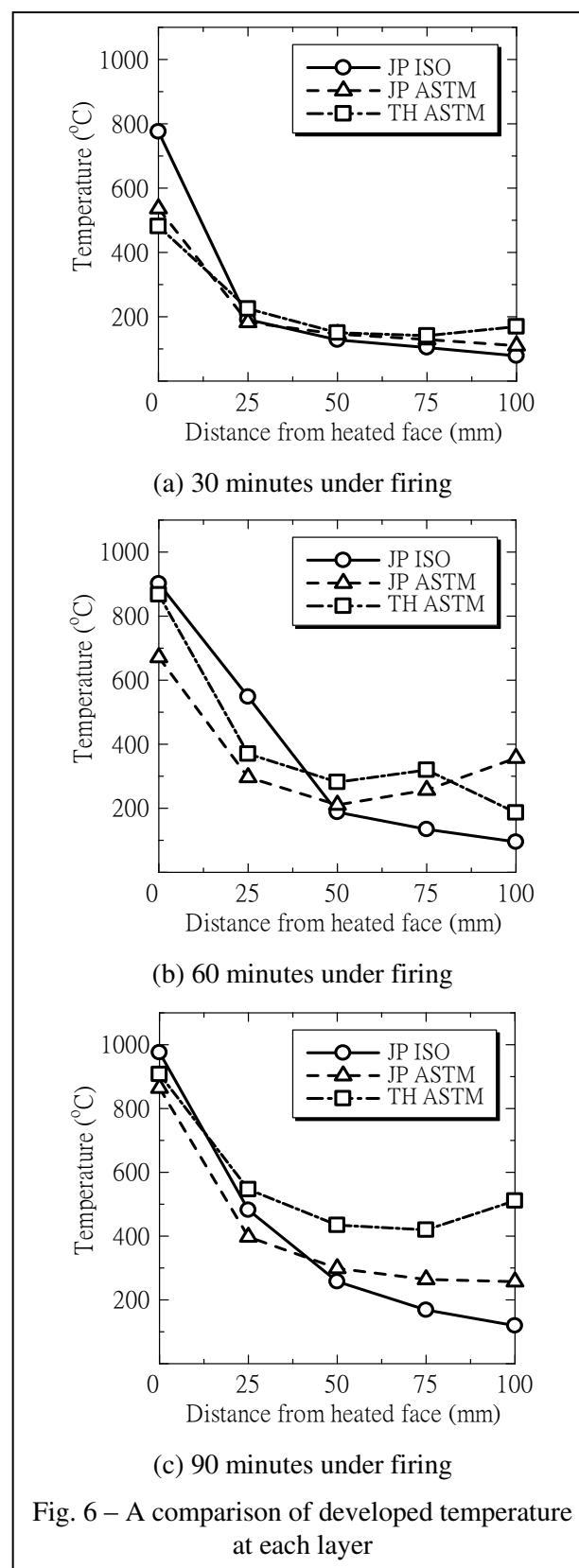


Fig. 6 – A comparison of developed temperature at each layer

history could be described by the different crack mappings.

3.2 Post-cooling visual observations

Although it has been reported in reference 14 that the different maximum temperatures to which specimens are exposed could introduce different

degrees of deterioration, no quantitative surface damage assessments have yet been reported. Therefore, we aimed to understand the general conditions of the specimens and the quantitative crack assessments of mortars after heating and cooling. In this study, there are two types of cracks: crazing on the heated face and cracking on side faces of the mortar prism. During exposure to fire, the heated face started cracking, with interconnections between cracks, and then crazing was finally found on the heated face in all series. Furthermore, some cracks on the side face were interconnected with the crazing on the heated face. This means that the damage evidence appearing on the heated face might not be simply aesthetic deterioration. Sometimes existing post-fire cracking may affect the material strength at the serviceability level.

The physical condition of the fire damaged specimens is shown in Fig. 7. One-directional fire exposure was applied to the heated face, which experienced a drastically increased temperature. Meanwhile, the temperature of the internal layer of mortar might have been comparatively low. This means that there was a large difference in temperature between the heated and unheated faces at the beginning of the burning process. This could cause an expansion at the heated face, without corresponding expansion of the other sides. In this study, all specimens were instantaneously cooled in air after reaching the target duration. As a result of this, the temperature to which mortars were exposed, especially at the heated face, changed suddenly. An expanded surface in the heating process might suddenly shrink. Therefore, relatively straight cracks were introduced perpendicular to the heated face owing to the decrease in tensile strength under high temperature, as well as the rapidly developed tensile stress [26].

From the overview of the physical damage conditions in all specimens, it is seen that the number of cracks increases with increasing time exposure. Moreover, the average length of these cracks tends to be higher for longer durations. To obtain a better understanding of this phenomenon, quantitative cracking assessments of the JP ISO series were conducted. Figure 8 shows the techniques of crack observations. The surface crack density at the heated face was determined by the number of interceptions of craze cracking on the virtual grid. Meanwhile, the crack depth and crack spacing were determined on both side faces. The crack density on the heated face, as illustrated in Fig. 9, tended to be higher for specimens that were exposed to higher temperatures.

However, the characteristics of cracks on the side faces were different from the crazing found on the heated surface. Relatively straight cracks were

seen on the side faces. The crack depth, which was measured from the edge of the side face to the tips of cracks, was not significantly different when comparing different cases and the distribution of spacing between single cracks became less scattered as the time exposure increased. The results of the crack depth and spacing are shown in Fig. 10(a) and 10(b), respectively. Although longer cracks could be observed when specimens were subjected to longer exposures, there is no clear relationship between average crack depth and exposure time. As seen from Fig. 10(b), the crack spacing could explain the progress of cracks more clearly. Because the mortar was allowed to cool down immediately in air, the external thermal loading at the heated face changed suddenly from high to ambient temperature. The increase in exposure time and temperature might cause more expansion in the mortar and decrease the resistance to crack initiation. Therefore, the number of cracks on the side faces is increased with increased exposure time. The high variance in the crack spacing is observed in mortar exposed to short-term firing, whereas scattering decreases with longer exposure.

The horizontal cracks are observed as well as perpendicular cracks, especially for siliceous mortar. In case of the calcareous mortars, the general cracking condition was approximately the same even when exposed to different firings. However, the horizontal cracking became more severe and the binding property was ruined in case of the siliceous mortar. The degree of this deterioration became more obvious after 90-minute exposure of siliceous mortar to heat. The characteristics of these horizontal cracks seem to indicate an expansion crack in firing. This difference in cracking pattern may reflect the significant difference in developed temperature gradients, as mentioned in section 3.1.

By comparing the developed temperature gradients along the cross section and the visual observations, it can be seen that the degree of deterioration of cementitious material progresses as exposure time, or temperature to which the mortar is exposed, increases. Moreover, the difference in raw materials used in mix proportions may be a key parameter for understanding general physical damage to cementitious materials exposed to fire, whose influences will be discussed elsewhere. Based on the results of developed temperature and the crack assessments, the existence of fire cracks could demonstrate how fire deterioration progresses in cementitious material and must be taken into account to achieve the mechanical properties of fire damaged cementitious material more precisely [27,28].



Fig. 7 – Crack patterns on both sides of specimens

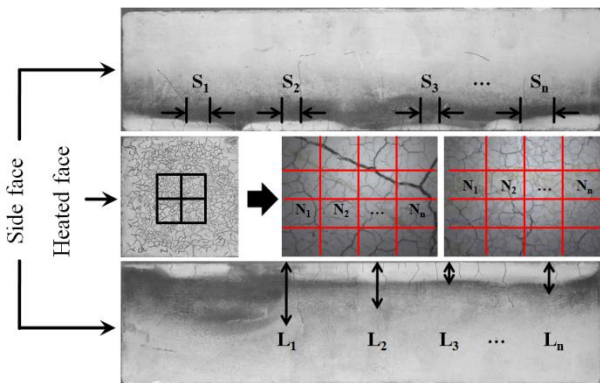


Fig. 8 – Crack observations of specimen's face

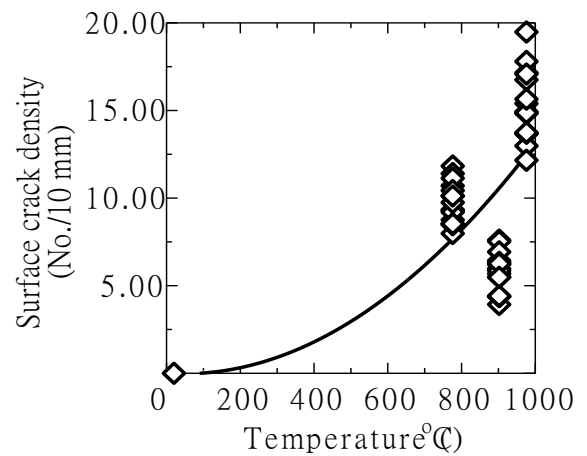
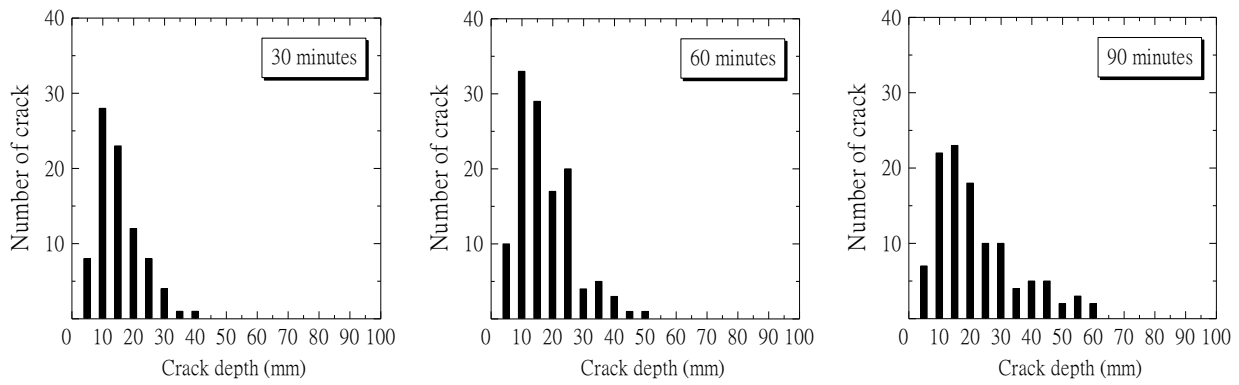
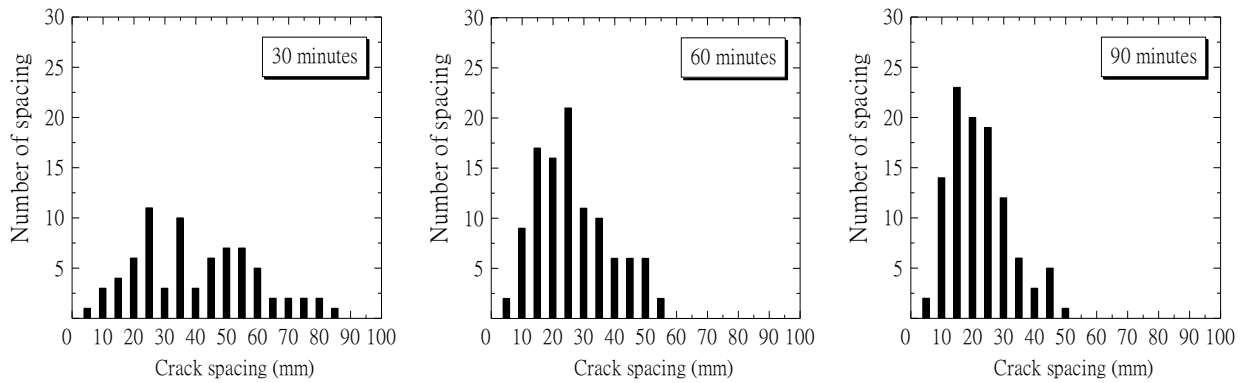


Fig. 9 – Surface crack density-temperature relation



(a) Crack depth



(b) Crack spacing

Fig. 10 – Crack observations on side face

3.3 Mesoscopic flexural test

The approximately 10-mm-thick testing specimens were prepared while avoiding straight visible cracks initiated by heating and cooling to measure the material strength along the beam depth after firing. However, visible cracks that propagated from the crazing at the heated face could be found on the bottom and top fiber of the thin specimens, especially for the specimens near the heated face. The damage evidence, i.e., visible cracks propagating from the crazing, still existed up to approximately 20 mm in case of 30-minute firing and 40 mm from heated face for 60- and 90-minute firings. The crack width, which ranged from 0.03 to 0.40 mm, was measured on the bottom and top faces of the thin specimens.

The flexural strength along the beam depth for all fire cases, including reference specimens, is illustrated in Fig. 11. The average flexural strength of non-damaged mortar was 7.20 N/mm², and this tended to be reduced in all fire-exposed specimens, especially for the layer that was directly exposed to fire at the bottom. The flexural strength of those layers was reduced by 66%, 72%, and 81% of non-damaged strength for 30, 60, and 90 minutes under firing, respectively. The loss of flexural strength of

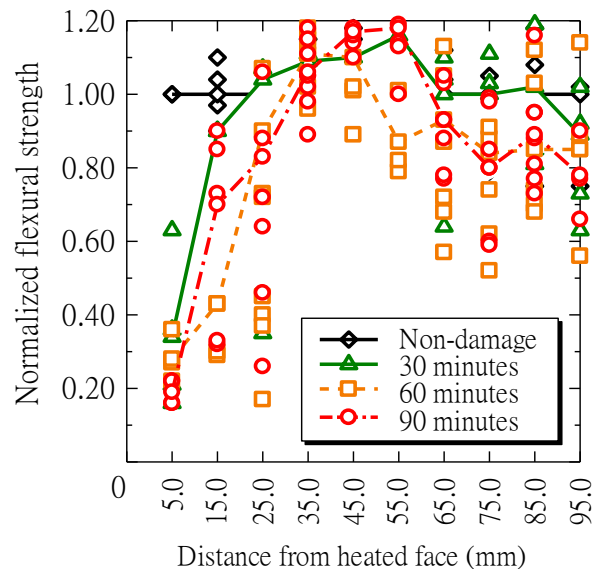


Fig. 11 – Meso scale flexural strength

those layers was not significantly different when compared between cases because the existing crack caused a weak point and a bending failure location. At a greater distance from the heated surface, the visible damage disappeared. Therefore, the flexural strength gradually became similar to the flexural strength of the non-damaged material. Based on the

measurements of flexural strength, the loss in strength was up to approximately 30 mm from the heated face, the same as the existence of damage evidence on the surface of the thin specimens. Therefore, the influence of cracking on post-fire material strength should be taken into account. We also observed a slight increase in strength in some layers next to the severely damaged zone. This is probably because of the rehydration of the unhydrated cement particles within the appropriate range of temperature.

In the flexural test, the failure modes could be divided into two categories, as shown in Fig. 12. The pre-existing crack was vertically set at the front and back sides along the thin specimen's thickness. When applying a single point load at the top fiber up to the load limit, a real crack would occur. The bending failure locations of non-damaged specimens and specimens without visible cracks were usually found at pre-existing cracks, as illustrated in Fig. 12(a). On the other hand, the bending failure location was dependent upon the location of major fire crack, as shown in Fig. 12(b). Therefore, mortar exposed to fire shows structural deterioration, especially for specimens containing cracks induced by fire.

Fire exposure is related to thermal loading. Therefore, temperature is probably one of the appropriate primary indices for predicting the fire damage characteristics of cementitious material. Several studies [11,12] have investigated the effect of temperature background on fire-damaged material properties. Figure 13 shows the compressive strength of normal weight concrete at elevated temperature which is reported in Eurocode [29]. It was diminished with respect to an increase in temperature in both siliceous and calcareous aggregates. However, there is no report regarding the influence of fire cracks on those material properties.

Figure 14 shows the relation between flexural strength and temperature. In the early stage of burning, the flexural strength is slightly increased compared with the strength without any damage. After that, a rapidly decreasing gradient is observed. With respect to an increase in temperature, the flexural strength would be more scattered because of the existence of cracks induced by fire. The flexural strength-temperature relation is slightly different from that of the Eurocode because the existence of a fire crack has been taken into account and the meso-scale damage assessment could obtain the post-fire properties more precisely than conventional methods of evaluation.

In addition to the flexural strength, the modulus of elasticity and theoretical fracture energy, based on the concept of the RILEM recommendation [30], could be determined from the experi-



(a) For non-damaged specimen and specimen without fire crack



(b) For specimen with existing fire crack

Fig. 12 – Bending failure locations

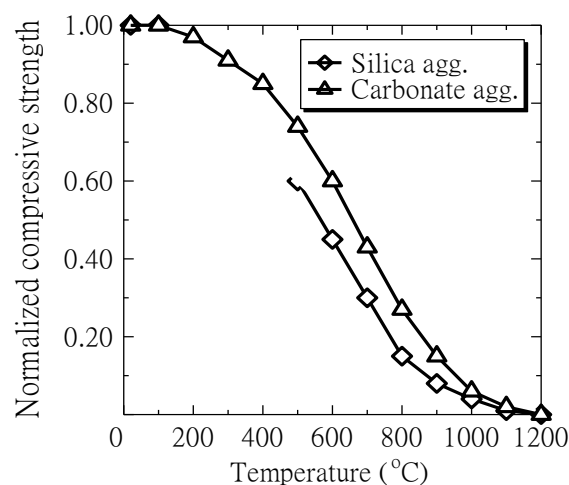


Fig. 13 – Variation of compressive strength at elevated temperature by Eurocode [29]

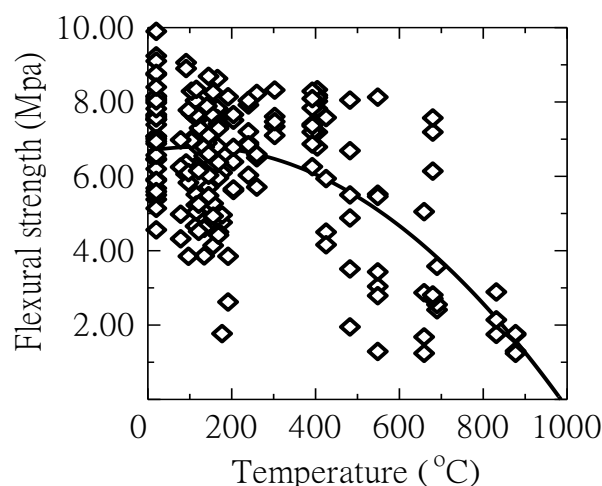


Fig. 14 – Flexural strength-temperature relation

mental data of the 3-point bending test, as shown in Eqs. (4), (5), and (6), respectively. Figure 15 shows the average modulus of elasticity along the beam depth. The result shows that the severely damaged zone could be observed as being the same as the flexural strength. When the distance from the heat-

ed face is increased, the modulus of elasticity would be increased. However, it is supposed to decrease with thermal experience from the non-damaged specimen.

$$E = \frac{P_{1/3} \cdot L^3}{4 \cdot \delta_{1/3} \cdot b \cdot h^3} \quad (4)$$

$$G_f = \frac{W_0 + W_1}{A_{lig}} \quad (5)$$

$$W_1 = \left(\frac{L_s}{L} \cdot m_1 + 2 \cdot m_2 \right) \cdot N \cdot \delta_{tu} \quad (6)$$

where E represents Young's modulus; $P_{1/3}$ and $\delta_{1/3}$ are loading (N) and displacement (mm), respectively, at one-third of the peak load. To calculate the fracture energy (G_f), the area under the load-deflection curve (W_0), cross-sectional area at mid-span (A_{lig}), length of the specimen (L_s), span length (L), dead weight (m_1), weight of equipment (m_2), gravitational acceleration (N), and displacement at 2 N of the descending branch (δ_{tu}) are required.

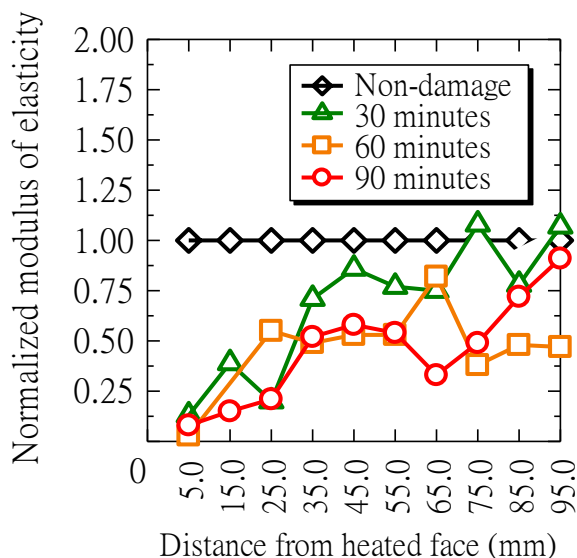


Fig. 15 – Modulus of elasticity

As for the flexural strength, the relationship between the modulus of elasticity and temperature can be discussed as shown in Fig. 16. It can be seen that, as for flexural strength, the modulus of elasticity is strongly related to temperature experiences. Therefore, both are supposed to have a mutual relation. Figure 17 shows the relationship between the modulus of elasticity and flexural strength. An obvious decrease in the modulus of elasticity can be seen when the flexural strength was also comparatively low, i.e., the flexural strength of specimens with an existing fire crack. However, the modulus

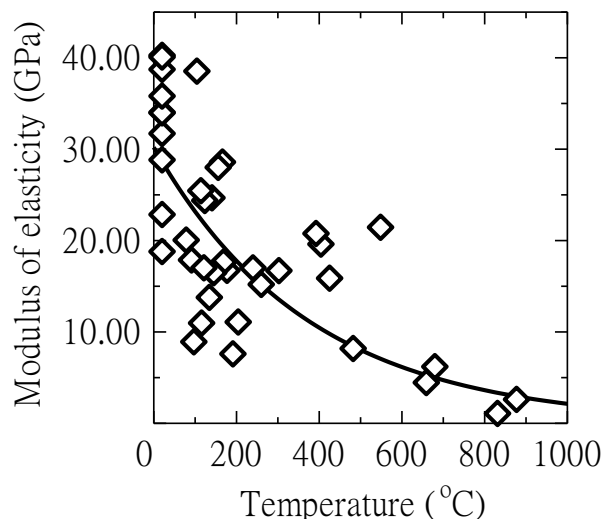


Fig. 16 – Modulus of elasticity-temperature relation

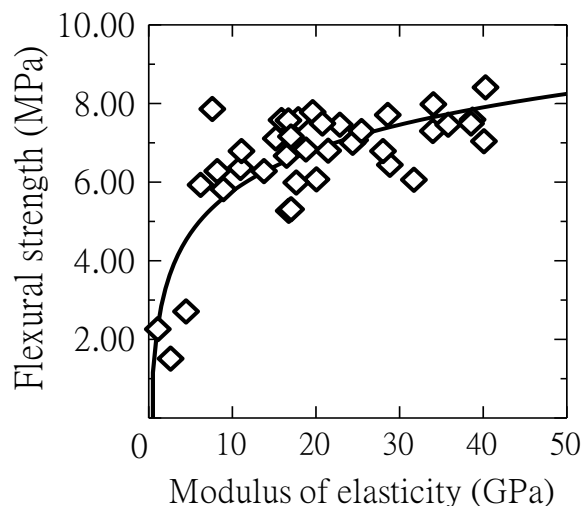


Fig. 17 – Flexural strength-modulus of elasticity

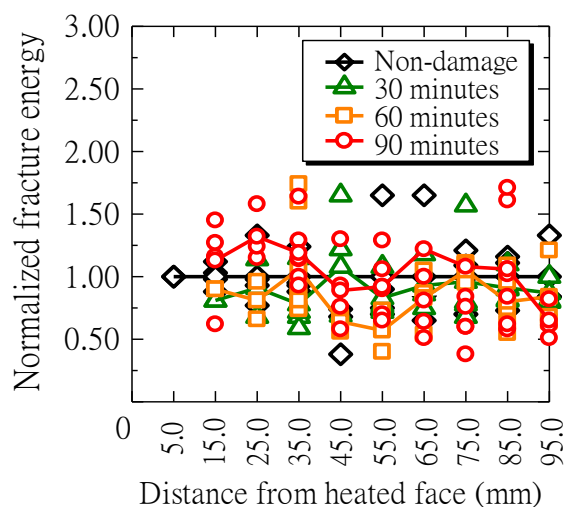


Fig. 18 – Theoretical fracture energy

of elasticity of thermal-experienced specimens was also decreased, even though the flexural strength was similar to that of the non-damaged material.

Because both the flexural strength and modulus of elasticity of the mortar were substantially diminished, especially for specimens with existing fire cracks, a precise material model to predict the mechanical properties of fire-damaged cementitious material must consider the effect of cracking induced by fire exposure.

The result of fracture energy, G_f , calculated based on the concept of the RILEM recommendation, is illustrated in Fig. 18. The average G_f of the non-damaged series is 24.78 N/mm. According to the results, the fracture energy of all fire-damaged series was not significantly different compared with that of the reference specimens.

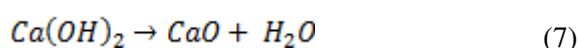
3.4 Residual hydration products

When the mortar is exposed to fire, a high temperature could introduce a change in the molecular structure of the chemical composition, i.e., the liberation of chemically bound water. In this study, only calcium hydroxide (CH) and calcium silicate hydrate (CSH), which are known to have an influence on a material's performance and its durability, are discussed. During firing, the compounds still exist up to a certain temperature, i.e., approximately 450-500 °C for CH [9] and 500-550 °C for CSH [11], while the rehydration process could regenerate in the early stage of burning. The authors would like to determine the residual chemical contents at the location where the temperature is sufficiently high for decomposition, as well as the location where the material strength has been recovered. In this study, the residual chemical compounds refer to the remaining amount in specimens after heating and cooling.

3.4.1 Calcium hydroxide (CH)

There is a molecule of water in the chemical structure, i.e., $\text{Ca}(\text{OH})_2$, which could be vaporized at a high temperature, as demonstrated in Eq. (7). This concept was used in TG/DTA to determine the remaining amount of CH in the powder based on the law of mass conservation.

The results of the remaining amount of CH in Fig. 19 could describe the reduction tendency along the beam depth, especially in the directly heated layer. The amount of CH was reduced by 51%, 67%, and 65% compared with the non-damaged specimen after 30, 60, and 90 minutes under firing, respectively. The average temperatures of 659 °C, 831 °C, and 877 °C for each case are sufficiently high for the decomposition of those layers. At a greater distance from heated face, the residual amount of CH tends to be higher.



3.4.2 Calcium silicate hydrate (CSH)

Calcium silicate hydrate or CSH has a complex molecular structure, including a molecule of water, which could be liberated at a high temperature as in calcium hydroxide. Therefore, it should be decomposed during fire exposure. Generally, CSH can be dissolved in a solution made from methanol and salicylic acid. By using this technique, the residual amount of CSH can be experimentally examined.

The result shown in Fig. 20 clearly indicates that CSH decomposition occurred in all fire-exposed specimens. In the layer that was directly heated at the bottom fiber, CSH was decomposed by 29%, 63%, and 55%, compared with the non-damaged specimen after 30, 60, and 90 minutes under firing, respectively. A substantial decrease in CSH could also be observed even at greater distances from the heated side.

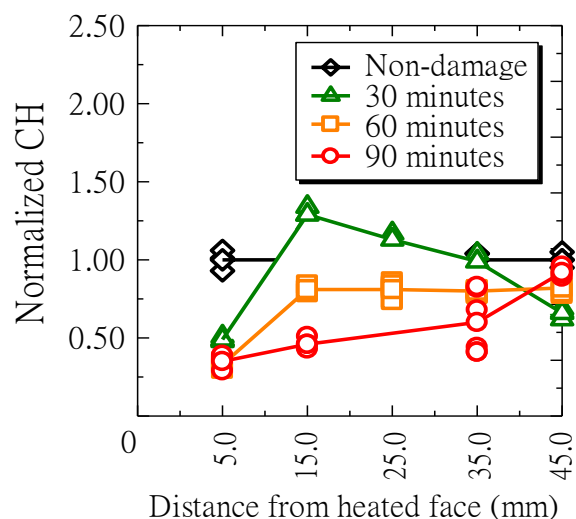


Fig. 19 – Residual amount of CH

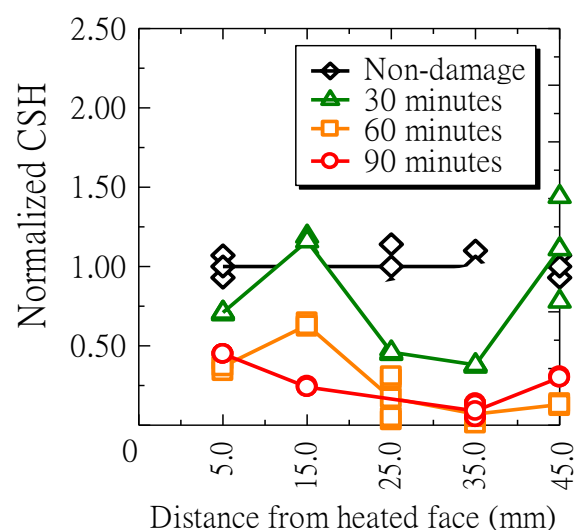
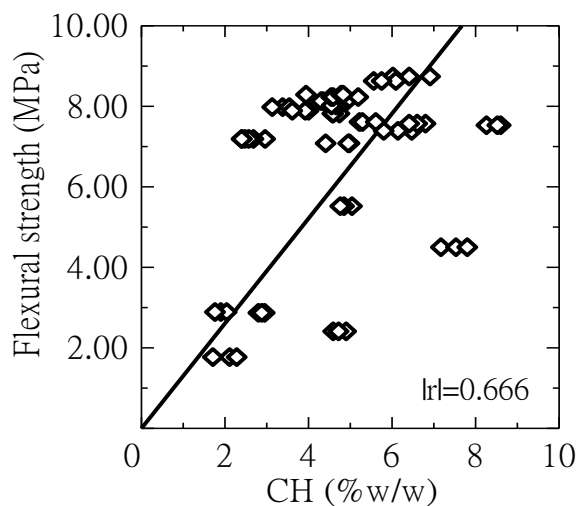
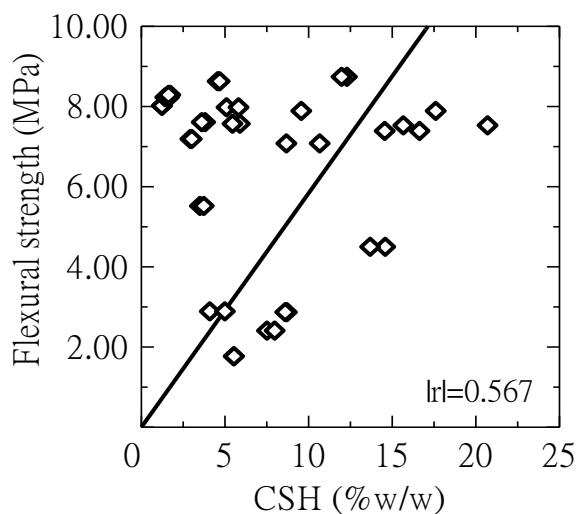


Fig. 20 – Residual amount of CSH

To understand the effect of cement hydrates on the mechanical strength of fire-deteriorated cementitious material, the relationships between chemical compounds and flexural strength are shown in Fig. 21(a) and Fig. 21(b) for CH and CSH, respectively. The individual relation of each chemical compound to flexural strength does not show a clear tendency. However, the integration of the decomposed amount of chemical compounds also does not clearly describe the loss in flexural strength. Moreover, the change in porosity caused by the chemical decomposition is mainly affected by the calcium leaching, not by the evaporation of chemically bound water from the molecular structure. Consequently, the individual influence of porosity and the physico-chemical characteristics might not have a strong relation with the mechanical characteristics of cementitious material in the fire problem.



(a) Flexural strength-CH relation



(b) Flexural strength-CSH relation

Fig. 21 – Flexural strength-chemical compounds relations

3.5 Porosity by water absorption

Approximately $10 \times 10 \times 10$ mm cubes were picked from both sides of the thin specimens beyond the bending crack after testing. To obtain an overview of the changes in porosity, the authors would like to describe the porosity trends induced by short and long durations of firing. Figure 22 shows that the porosity along the beam depth of fire-damaged specimens is not significantly different compared with reference series. Because the porosity test was conducted on the post-cooling specimens, additional cement hydrates [10,26,31], as well as existing fire cracks, could affect the porosity value. Therefore, porosity might not be an appropriate index for understanding the material strength of fire-damaged mortar. Although the fire did not introduce a change in porosity value, it might introduce a change in pore structure in other ways, such as pore structure coarsening.

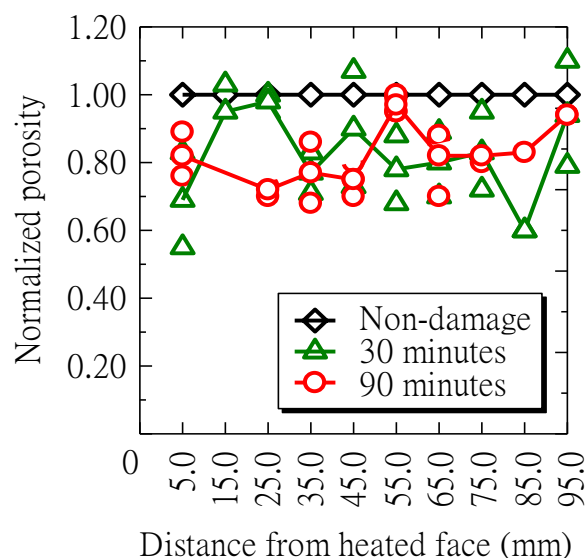


Fig. 22 – Porosity by water absorption

Instead of the expected increasing trend in the relationship between porosity and temperature due to chemical decomposition, the porosity did not show a strong relation with temperature, as demonstrated in Fig. 23, as for the mechanical properties, i.e., flexural strength and modulus of elasticity. Therefore, porosity is not a good index for understanding the strength of cementitious material in the fire problem.

In fact, all fire damage characteristics, including the decrease in material strength leading to the initiation and propagation of cracks and chemical decomposition leading to a change in pore structure, were initiated by high temperature. The temperature experience is therefore the most appropriate index, with wide applicability, for understanding the residual mechanical properties of fire-damaged cementitious materials.

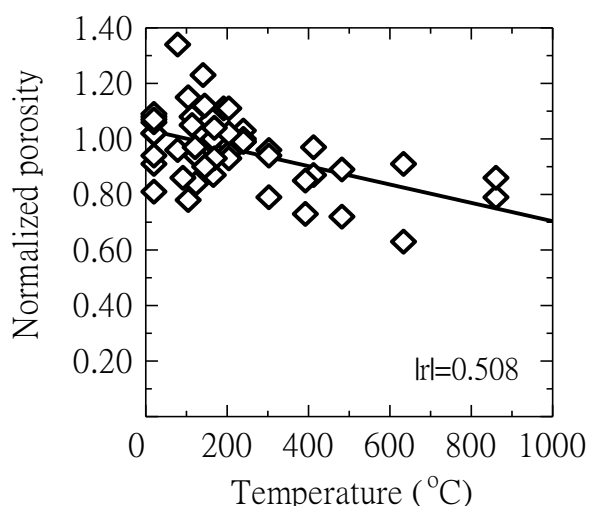


Fig. 23 – Porosity-temperature relation

4. Conclusions

The conclusions drawn from the experimental results obtained in this study are as follows:

- (1) All of the experimental results, including mechanical characteristics, porosity, and chemical compositions, show non-uniform distribution of the degree of fire deterioration, which is dependent upon the distance from the fire origin. This finding implies that assessment at a small scale can describe fire damage characteristics more precisely than a macro-scale structural response.
- (2) The relationships between material strength and chemical compositions show that they are not able to describe the reduction of strength and stiffness of fire-damaged mortar, while the porosity after heating and cooling also does not have clear tendency. In addition, the crack induced by fire which has a stronger effect to the material strength and failure mode can also be treated as a kind of porosity. Therefore, the porosity and hydration products are inappropriate indices for cementitious material in fire problem.
- (3) According to the strong relationships of mechanical characteristics and temperature, as well as the crack assessments, the temperature is the most appropriate index to describe how the damage of cementitious material in fire problem progresses and to understand the post-fire mechanical properties, and it could be involved in all aspects of damage.
- (4) Because of the strong influence of the existence of fire cracks on mechanical behavior of post-fire mortar, the cracks must be taken into account in order to achieve the strength and

stiffness more precisely. Therefore, the relationship between mechanical properties and temperature experiences, considering the effect of fire crack is powerful and has a wide applicability range. In addition, the influence of fire crack on mechanical properties implies that the cementitious material with different fire crack characteristics could have different mechanical responses.

Acknowledgements

The authors gratefully acknowledge the Hokkaido Northern Regional Building Research Institute in Asahikawa, Japan, and Laboratory of Fire Resistance, Chulalongkorn University, Thailand, who supplied the fire furnace and raw materials for making mortar in this study.

References

1. Siam Cement Group, Co., Ltd. (2009) Cement and Applications, Bangkok, Thailand. (*in Thai*.)
2. Xu, Y.; Wong, Y. L.; Poon, C. S.; and Anson, M. (2001) "Impact of high temperature on PFA concrete," *Cement and Concrete Research*, 31, pp. 1065-1073.
3. Husem, M. (2006) "The effects of high temperature on compressive and flexural strengths of ordinary and high-performance concrete," *Fire Safety Journal*, 41, pp. 155-163.
4. Vichit-Vadakan, W. and Elizabeth A. K. (2009) "Transport properties of fire-exposed concrete," *Journal of Advanced Concrete Technology*, 7(3), pp. 393-401.
5. Belkacem, T. and Musa, R. (2010) "Influence of high temperature on surface cracking of concrete studied by image scanning technique," *Jordan Journal of Civil Engineering*, 4(2), pp. 155-163.
6. Heikal, M. (2000) "Effect of temperature on the physico – mechanical and mineralogical properties of Homra pozzolanic cement pastes," *Cement and Concrete Research*, 30, pp. 1835-1839.
7. Rongviriyapanich, O.; Pansuk, W.; and Sato, Y. (2013) "Effect of chemical compound reduction on oven – dried mortar subjected to elevated temperature," *The 18th National Convention on Civil Engineering*, Chiangmai, Thailand, pp. 58-63.
8. Rostasy, F. S.; Weib, R.; and Weidemann, G. (1980) "Changes in pore structure of cement mortars due to temperature," *Cement and Concrete Research*, 10, pp. 157-164.
9. Piasta, J.; Sawicz, Z.; and Rudzinski, L. (1984) "Changes in the structure of hardened cement paste due to high temperature," *Material Construction*, 17, pp. 291-296.
10. Lin, W. M.; Lin, T. D.; and Powers-Couche, L. J. (1996) "Microstructures of fire-damaged concrete," *ACI Materials Journal*, pp. 199-205.
11. Peng, G. F. and Huang, Z. S. (2008) "Change in microstructure of hardened cement paste subjected to elevated temperatures," *Construction and Building Materials*, 22, pp. 593-599.

12. Chang, Y. F.; Chen, Y. H.; Sheu, M. S.; and Yao G. C. (2006) "Residual stress-strain relationship for concrete after exposure to high temperatures," *Cement and Concrete Research*, 36, pp. 1999-2005.
13. Chen, X. D.; Wu, S. X.; and Zhou, J. K. (2013) "Influence of porosity on compressive and tensile strength of cement mortar," *Construction and Building Materials*, 40, pp. 869-874.
14. Arioiz, O. (2007) "Effects of elevated temperature on properties of concrete," *Fire Safety Journal*, 42, pp. 516-522.
15. Poon, C. S.; Azhar, S.; Anson, M.; and Wong, Y. L. (2001) "Strength and durability recovery of fire-damaged concrete after post-fire-curing," *Cement and Concrete Research*, 31, pp. 1307-1318.
16. Tencheve, R. T.; Li, L. Y.; and Purkiss, J. A. (2001) "Finite element analysis of coupled heat and moisture transfer in concrete subjected to fire," *Numerical Heat Transfer, Part A*, 39, pp. 685-710.
17. Djaknoun, S.; Ouedraogo, E.; and Benyahia, A. A. (2012) "Characterisation of the behavior of high performance mortar subjected to high temperature," *Construction and Building Materials*, 28, pp. 176-186.
18. Bessey, G. E. (1950) "Investigations on Building Fires, Part II: the visible changes in concrete or mortar exposed to high temperatures," *National Building Studies Technical Paper*, 4, pp. 6-18.
19. Hertz, K. D. (2003) "Limits of spalling of fire-exposed concrete," *Fire Safety Journal*, 38, pp. 103-116.
20. Georgali, B. and Tsakiridis, P. E. (2005) "Microstructure of fire – damaged concrete. A case study," *Cement and Concrete Composites*, 27, pp. 255-259.
21. Daungwilailuk, T. (2013) Assessment of fire – damaged concrete, Master Thesis, Faculty of Engineering, Chulalongkorn University, Bangkok, Thailand. (*in Thai*.)
22. Fu, Y. F.; Wong, Y. L.; Poon, C. S.; Tang, C. A.; and Lin, P. (2004) "Experimental study of micro/macro crack development and stress-strain relations of cement-based composite materials at elevated temperatures," *Cement and Concrete Research*, 34, pp. 789-797.
23. Nakamura, H.; Yoshida, K.; Kunieda, M.; Ueda, N.; and Yamamoto, Y. (2011) "Simulation about effect on explosion spalling of thermal stress and vapor pressure," 2nd International RILEM Workshop on Concrete Spalling due to Fire Exposure, Delft, The Netherlands, pp. 213-219.
24. Sato, Y.; Miura, T.; and Nakamura, H. (2015) "Me-so-scale analysis of the mechanical properties of chemically-deteriorated mortar" The 10th International conference on mechanics and physics of creep, shrinkage, and durability of concrete and concrete structures, Vienna, Austria, pp. 1251-1258.
25. Abdulkareem, O. A.; Mustafa Al Bakri, A. M.; Kamarudin, H.; Nizar, I. K.; and Saif, A. A. (2014) "Effects of elevated temperatures on the thermal behavior and mechanical performance of fly ash geopolymer paste, mortar and lightweight concrete," *Construction and Building Materials*, 50, pp. 377-387.
26. Yuzer, N.; Akoz, F.; and Ozturk, L. D. (2004) "Compressive strength-color change relation in mortars at high temperature," *Cement and Concrete Research*, 34, pp. 1803-1807.
27. Rongviriyapanich, O.; Sato, Y.; and Pansuk, W. (2014) "The observations of aesthetic damage to oven-dried mortar exposed to fire," The 6th Asia and Pacific Young Researchers and Graduates Symposium, Pathumthani, Thailand, pp. 144-148.
28. Rongviriyapanich, O.; Sato, Y.; and Pansuk, W. (2014) "Assessment of surface cracks and temperature on post-fire mortar," The 16th International Summer Symposium of Japan Society of Civil Engineers (JSCE), Osaka, Japan, pp. 119-120.
29. EC2 (2004) Eurocode 2: design of concrete structures - part 1.2: general rules structural fire design, European Committee for Standardization.
30. RILEM Draft Recommendation (1985) "Determination of the fracture energy of mortar and concrete by means of three-point bend tests on notched beams materials and structures," 18, pp. 285-290.
31. Heap, M. J.; Lavalley, Y.; Laumann, A.; Hess, K. U.; Meredith, P. G.; Dingwell, D. B.; Huisman S.; and Weise, F. (2013) "The influence of thermal-stressing (up to 1000 °C) on the physical, mechanical, and chemical properties of siliceous-aggregate, high-strength concrete," *Construction and Building Materials*, 42, pp. 248-265.